Epigenetic Silencing of *CRABP2* and *MX1* in Head and Neck Tumors[1,2]

Marilia F. Calmon[*,3], Rodrigo V. Rodrigues[†,‡,3], Carla M. Kaneto[§], Ricardo P. Moura[¶], Sabrina D. Silva[#], Louise Danielle C. Mota[#], Daniel G. Pinheiro[§], Cesar Torres[#], Alex F. de Carvalho[#], Patrícia M. Cury[†], Fabio D. Nunes[**], Ines Nobuko Nishimoto[#], Fernando A. Soares[#], Adriana M.A. da Silva[††], Luis P. Kowalski[#], Helena Brentani[#], Cleslei F. Zanelli[‡‡], Wilson A. Silva Jr.[§], Paula Rahal[*], Eloiza H. Tajara[†,‡], Dirce M. Carraro[#], Anamaria A. Camargo[¶] and Sandro R. Valentini[‡‡]

*Department of Biology, IBILCE-UNESP, São José do Rio Preto–SP, 15091-450, Brazil; †Department of Molecular Biology, School of Medicine–FAMERP, São José do Rio Preto–SP, 15090-000, Brazil; ‡Department of Genetics and Evolutionary Biology, Institute of Biosciences–USP, São Paulo–SP, 05508-090, Brazil; §Department of Genetics, School of Medicine–USP, Ribeirão Preto–SP, 14051-140, Brazil; ¶Ludwig Institute for Cancer Research at Oswaldo Cruz Hospital, São Paulo–SP, 01323-903, Brazil; #A.C. Camargo Cancer Hospital–Medical and Research Center, São Paulo–SP, 01509-900, Brazil; **School of Dentistry–USP, São Paulo–SP, 05508-000, Brazil; ††Heliópolis Hospital, São Paulo–SP, 04231-030, Brazil; ‡‡Department of Biological Sciences, School of Pharmaceutical Sciences–UNESP, Araraquara–SP, 14801-902, Brazil

Abstract

Head and neck squamous cell carcinoma (HNSCC) is a heterogeneous disease affecting the epithelium of the oral cavity, pharynx and larynx. Conditions of most patients are diagnosed at late stages of the disease, and no sensitive and specific predictors of aggressive behavior have been identified yet. Therefore, early detection and prognostic biomarkers are highly desirable for a more rational management of the disease. Hypermethylation of CpG islands is one of the most important epigenetic mechanisms that leads to gene silencing in tumors and has been extensively used for the identification of biomarkers. In this study, we combined rapid subtractive hybridization and microarray analysis in a hierarchical manner to select genes that are putatively reactivated by the demethylating agent 5-aza-2′-deoxycytidine (5Aza-dC) in HNSCC cell lines (FaDu, UM-SCC-14A, UM-SCC-17A, UM-SCC-38A). This combined analysis identified 78 genes, 35 of which were reactivated in at least 2 cell lines and harbored a CpG island at their 5′ region. Reactivation of 3 of these 35 genes (*CRABP2*, *MX1*, and *SLC15A3*) was confirmed by quantitative real-time polymerase chain reaction (PCR; fold change, ≥3). Bisulfite sequencing of their CpG islands

revealed that they are indeed differentially methylated in the HNSCC cell lines. Using methylation-specific PCR, we detected a higher frequency of *CRABP2* (58.1% for region 1) and *MX1* (46.3%) hypermethylation in primary HNSCC when compared with lymphocytes from healthy individuals. Finally, absence of the CRABP2 protein was associated with decreased disease-free survival rates, supporting a potential use of CRABP2 expression as a prognostic biomarker for HNSCC patients.

Neoplasia (2009) 11, 1329–1339

Introduction

Head and neck squamous cell carcinoma (HNSCC) comprises a heterogeneous disease, which arises from the epithelium of the oral cavity, pharynx, and larynx [1], and is associated with tobacco and alcohol abuse [2]. According to worldwide cancer statistics, approximately 450,000 new oral and laryngeal carcinomas are diagnosed annually, and the incidence varies between countries, probably as a result of environmental risk factors [3]. For example, the incidence rates for oral cancer in males are high in France and comparatively low in the United States and Brazil [4–6].

Although detection of HNSCC in early stages improves the survival rate, most patients present advanced stages of the disease at the time of diagnosis, and no sensitive and specific predictors of aggressive behavior have been identified. Lymph node status is still the most powerful prognostic factor, but the routine histopathologic examination of neck dissection specimens is unable to detect all micrometastases [7]. Therefore, the identification of early detection and prognostic biomarkers is highly desirable for planning an efficient and appropriate treatment procedure.

Evidence for a fundamental role for epigenetic modifications in head and neck cancer cells has been widely reported in the literature, including DNA methylation and histone deacetylation [8,9]. Both promoter hypermethylation of specific genes [10–12] and global hypomethylation are implicated in head and neck tumorigenesis [13,14].

Aberrant DNA methylation, such as regional gains or global loss, is an early event that occurs as a nonrandom signature in almost all tumors [15] and may be used for the identification of biomarkers. Strategies for assessing genome-wide methylation changes include genomic scanning after methylation-specific cleavage of the DNA and two-dimensional electrophoresis, amplification of intermethylated sites by arbitrarily primed polymerase chain reaction (PCR), and microarray gene expression analysis after treatment with DNA demethylating agents such as the DNA methyltransferase inhibitor 5-aza-2′-deoxycytidine (5Aza-dC) [16,17]. 5Aza-dC is incorporated into genomic DNA during replication, where it acts as an irreversible inhibitor of methyltransferase by forming a covalent complex with methyltransferase active sites. This suicide inhibition depletes methyltransferase activity, resulting in generalized DNA demethylation and release of specific genes from methylation-mediated transcriptional silencing [18].

In the present study, we carried out a genome-wide screening of 5Aza-dC–reactivated genes in four human squamous cell carcinoma cell lines derived from different topographical sites, using a combination of rapid subtractive hybridization (RaSH) and complementary DNA (cDNA) microarray analysis. This analysis revealed two genes reactivated by 5Aza-dC (*CRABP2* and *MX1*), and they were frequently hypermethylated in primary HNSCCs. Furthermore, the absence of CRABP2 protein was associated with decreased disease-free survival rates, supporting a potential use of CRABP2 expression as a prognostic biomarker for HNSCC.

Materials and Methods

Tumor Cell Lines and 5Aza-dC Treatment

Four HNSCC cell lines derived from distinct topographical sites, pharynx (FaDu), floor of the mouth (UM-SCC-14A), supraglottis (UM-SCC-17A), and tonsil (UM-SCC-38A), were used in this study. UM-SCC-14A, UM-SCC-17A, and UM-SCC-38A cell lines were kindly provided by Dr. Thomas E. Carey of the University of Michigan, USA, and FaDu (HTB-43) was purchased from American Type Culture Collection (ATCC, Manassas, VA). Cell lines were routinely cultured as monolayers in minimum essential medium (Eagle) supplemented with 10% fetal calf serum, 1% L-glutamine, and 1% penicillin/streptomycin, at 37°C and 5% carbon dioxide. Cells were seeded at a density of 10^6 cells/10-cm dish, cultured for 48 hours, and treated for 4 days with freshly prepared 2.5 µM 5Aza-dC (Sigma, St Louis, MO) dissolved in 50% acetic acid.

Tumor Samples

For methylation-specific PCR (MSP) analysis, 140 HNSCC samples and 10 lymphocyte samples from normal individuals were used. The samples were obtained from the Tumor Tissue Biobank of the Medical and Research Center – A.C. Camargo Hospital, São Paulo, and from the Head and Neck Genome Project/Gencapo – Brazil after Institutional Ethics Committee approval. Tumor samples were microdissected to enrich for tumor cells. Five-micrometer-thick sections from the frozen tumors were cut onto glass slides, fixed, and stained with hematoxylin and eosin. The hematoxylin and eosin–stained section was used as a guide for manual dissection, and only samples with more than 70% of tumor area were used in this study. All samples were reviewed by two independent pathologists. The main clinicopathological characteristics corresponding to these samples are shown in Table W3. None of the patients received preoperative treatment, and 41.3%, 42.0%, and 16.7% of patients were treated by surgery alone, surgery + radiotherapy, or surgery + radiotherapy + chemotherapy, respectively. The mean follow-up for these patients was approximately 31 months.

For the tissue microarray (TMA) analysis, an independent set of 75 HNSCC samples was used. These samples were obtained from the archives of the Department of Anatomic Pathology, A.C. Camargo Hospital, São Paulo, Brazil, and were reviewed by two independent pathologists. The main clinicopathological characteristics corresponding to these samples are also shown in Table W3. None of the patients received preoperative treatment, and 41.3%, 42.0%, and

6.7% of patients were treated by surgery alone, surgery + radiotherapy, or surgery + radiotherapy + chemotherapy, respectively. The average follow-up period was approximately 56 months.

DNA and RNA Extraction

Genomic DNA from tumor cell lines was purified using a Super Quick Gene DNA Isolation kit (Analytical Genetic Testing Center) following the protocol instructions. Total RNA was isolated using TRIzol Reagent for Molecular Biology (Invitrogen/Life Technologies, Carlsbad, CA). Genomic DNA from tumor samples was purified by standard phenol/chloroform purification. DNA quality was verified by electrophoresis through agarose gel on visualization with ethidium bromide. For microarray experiment, total RNA was further purified using the RNeasy Mini Kit (Qiagen, Valencia, CA). For quantitative real-time PCR (qRT-PCR), 5 μg of total RNA was previously treated with the RQ1 RNase-free DNase (Promega, Madison, WI). The RNA integrity after the purification procedure was evaluated using the Agilent 2100-Bioanalyser revealing a minimal RIN value of 7.9.

Rapid Subtractive Hybridization

RaSH cDNA libraries were prepared by a modified protocol taken from Jiang et al. [19]. The cDNA were initially digested with *Mbo*I (Gibco, Gaithersburg, MD) at 37°C for 1 hour. The fragments were inserted into *Xho*I-digested pZERO plasmid (1 μg/μl) at 16°C for 3 hours. The constructs were introduced into the DH10-B competent cells. Two RaSH cDNA libraries were prepared: one using cDNA from the FaDu cell line treated with 5Aza-dC as tester and the mock-treated FaDu cell line as driver and the other using cDNA from the mock-treated FaDu cell line as tester and cDNA from the FaDu cell line treated with 5Aza-dC as driver.

Bacterial colonies were selected randomly and PCR amplified, using M13 forward and reverse primers. Inserts were sequenced with forward and reverse M13 primers using a DYEnamic ET Dye Terminator Sequencing kit (Amersham Biosciences, Piscataway, NJ) and a MegaBACE 1000 sequencer (Amersham Biosciences). The sequences were analyzed, using an annotation pipeline that consists of four steps: 1) quality checking, phred base-calling, cutoff 0.05 [20,21]; 2) vector trimming and removal of undesirable sequences such as bacterial, mitochondrial, and rRNA sequences; 3) masking of repetitive elements and screening of low-complexity regions by Repeat Masker, using the default settings [22]; and 4) annotation against existing databases, using BLASTN with default parameters. Significant hits were determined by using an *E*-value threshold of 10^{-15} for searches against nucleotide sequence databases [23].

cDNA Microarray

A total of 151 RaSH cDNA clones were amplified by PCR, purified, and spotted onto glass slides (Corning, Corning, NY) with a Flexys Robot (Genomic Solutions, Ann Arbor, MI). A total of 2352 spots, including 151 RaSH cDNA clones, 496 negative controls (pure H_2O or DMSO), 48 positive controls (*Q gene* fragment from phage lambda), and 1657 cDNA fragments derived from other projects were arranged on this customized cDNA platform. Positive hybridization signals from all spots were considered for evaluation of hybridization quality, normalization, and statistical analysis. However, for the purpose of this study, only differences in the expression levels of RaSH cDNA clones were used.

Total RNA extracted from HNSCC cell lines was further purified using the RNeasy Mini Kit (Qiagen) before the RNA amplification procedure. A two-round RNA amplification procedure was carried out as previously described [24]. Amplified RNA was used in a reverse transcription reaction in the presence of random hexamer primer (Invitrogen/Life Technologies), Cy3- or Cy5-labeled dCTP (Amersham Biosciences), and SuperScript II (Invitrogen/Life Technologies). Equal amounts of Cy3- or Cy5-labeled cDNA derived from cell lines treated or not with 5Aza-dC were mixed and cohybridized to the customized platform. Dye swap was performed, and hybridizations were carried out in duplicates, resulting in four independent hybridizations for each cell line. Self-self hybridization experiments were performed by pooling the cDNA derived from the four untreated cell lines, labeling them with Cy3 and Cy5 independently. Labeled cDNA were then cohybridized to the customized platform. Dye swap was also performed, and hybridizations were carried out in duplicates, resulting in four independent hybridizations for self-self experiments. Arrays were scanned and extracted as previously described [25]. Self-self experiments–based statistical test for low-replication microarray studies was performed to select genes reactivated by 5Aza-dC treatment. This strategy has been used to derive intensity-dependent cutoffs to classify a gene as differentially expressed in microarray studies [26]. The cutoff for all comparisons between treated and untreated samples was 99%.

Selection of Genes for Validation by qRT-PCR

Genes that were reactivated by 5Aza-dC in at least two of the four cell lines and that possessed a CpG island in their 5′ region were selected for qRT-PCR validation. Genomic sequences corresponding to 5′ regions of reactivated genes were analyzed for the presence of a CpG island using the UCSC Genome Browser (http://genome.ucsc.edu/). Criterion for a CpG island was based on those of Gardiner-Garden and Frommer [27], as a GC content of 50% or greater, length greater than 200 bp, and a ratio greater than 0.6 of the observed number of CG dinucleotides to the expected number for the total number of Gs and Cs in the segment. Repeat Masker (ftp.genome.washington.edu/cgi-bin/Repeat-Masker) was used to determine whether selected CpG islands contained repetitive elements.

Quantitative Real-time Polymerase Chain Reaction

qRT-PCR amplification was performed with Power SYBR Green and an ABI 7500 Real-time PCR System (Applied Biosystems, Foster City, CA). The PCR total volume was 20.0 μl containing 10.0 μl of PCR Power SYBR Green Master Mix, 2.0 μl of diluted cDNA, and optimized primer concentrations for each primer pair (Table W4). Conditions were set as an initial polymerase activation step for 2 minutes at 50°C and 10 minutes at 95°C, followed by 40 cycles of 15 seconds at 95°C for template denaturation, 1 minute at 60°C for extension and fluorescence measurement. Afterward, a dissociation protocol was used for each primer pair to verify the specificity of the qRT-PCR reaction and the absence of primer dimer. All samples were amplified in triplicates and the mean was used for qRT-PCR analysis, and a no-template control was also included. Primers were located in different exons and designed for optimal hybridization kinetics with Primer Express 2.0 (Applied Biosystems). Relative quantification of gene expression was carried out with the mathematical model developed by Pfaffl [28]. All PCR efficiencies were greater than 95%. Non-treated cell lines were used as reference samples, and *TUBA1C* (*TUBA6*) was selected as endogenous control gene after GeNorm [29].

Bisulfite Sequencing

Genomic DNA was subjected to sodium bisulfite treatment to modify unmethylated cytosine to uracil, as previously described [30]. Hypermethylation in HNSCC cell lines was determined by the bisulfite sequencing. Bisulfite-treated DNA was amplified by a nested-PCR protocol, using primers designed to amplify CpG-rich regions located at the 5′ regions of *CRABP2* (–450 to –117 relative to transcription start site [TSS] encompassing 22 CpG dinucleotides), *MX1* (–71 to +845 relative to TSS encompassing 78 CpG dinucleotides), and *SLC15A3* (+351 to +845 relative to TSS encompassing 58 CpG dinucleotides; Figure 2). Primer sequences and PCR amplification conditions are available on request. Amplified products were cloned using the InsTAclone PCR Cloning Kit (Fermentas, Hanover, MD). Five positive clones were sequenced for each cell line using the Big Dye Terminator v3.1 Cycle Sequencing kit and an ABI3130 sequencer, in accordance with manufacturer's instructions (Applied Biosystems). The methylation percentage for each sample was calculated as the proportion of unconverted CpG dinucleotides among all the CpGs analyzed in all five positive clones.

Methylation-Specific PCR

Hypermethylation in head and neck tumors was determined by the MSP method as reported by Herman et al. [30], but amplified fragments were analyzed on silver-stained 8% polyacrylamide gels. Bisulfite-modified DNA was PCR amplified with primers specific for methylated *versus* unmethylated DNA. Two primer pairs were designed for MSP analysis of the *CRABP2* gene, and a single primer pair was used for the *MX1* gene, as indicated in Figure 2. Primer sequences and PCR amplification conditions are available on request.

Tissue Microarray

To construct the TMA, core biopsies were taken from previously defined areas, with a Tissue Microarrayer (Beecher Instruments, Silver Springs, MD). Tissue cores with a dimension of 1.0 mm were punched from each specimen and arrayed in duplicate on a recipient paraffin block. Each core was spaced 0.2 mm apart. After cutting (3 μm) on the recipient block and transferring with an adhesive tape to coated slides for subsequent UV cross-linkage (Instrumedics Inc, Hackensack, NJ), the slides were dipped in a layer of paraffin to prevent oxidation and kept in a –20°C freezer.

For immunostaining, the sections were deparaffinized and rehydrated in graded ethanol solutions, treated with peroxide to quench endogenous peroxidase (0.3% H_2O_2 for 15 min), and blocked for avidin/biotin (Biotin Blocking System; DAKO, Carpinteria, CA) and for protein (Protein Block Serum-Free; DAKO). Antigenic recovery was performed by wet heating in a pressure cooker. Slides were incubated with anti-CRABP2 (MAB5488, 1:2000; Chemicon, Inc, Temecula, CA). The immunohistochemical reaction was carried out in duplicate at different TMA levels, representing four-fold redundancy for each case. Positive and negative controls were included in all reactions. Positive controls were obtained using normal breast slides incubated with the CRABP2 antibody. CRABP2 binding was assessed by two kinds of negative controls: 1) omitting the primary antibody and incubating slides with phosphate-buffered saline; 2) replacing the primary antibody with normal mouse serum.

After scanning each tumor specimen in low power field to choose the most stained area, at least five fields were evaluated under high power. The presence of a clearly visible dark brown precipitation was considered an immunoreaction. Evaluation of CRABP2 included the proportion of reactive cells within the tumors and the staining intensity. The proportion score described the fraction of positively stained tumor cells (<10% of positive cells; ≥10% of tumors cells stained).

The immunostaining intensities were assessed visually by two pathologists using blind analysis by determining the color intensity of stained cells. The samples were classified as negative (no visible reaction or positivity in <10% of positive cells) or positive reaction (weak and strongly positive present in ≥10% of tumors cells stained). For statistical analysis, the samples were categorized into two groups: negative and weakly/strongly positive cases.

Statistical Analysis

For frequency analysis in contingency tables, statistical analyses of associations between variables were performed by the χ^2 test or Fisher's exact test (with significance set at $P < .05$). The overall survival was defined as the interval between the beginning of treatment and the date of death or the last information for censored observations. The disease-free interval was measured from the date of the treatment to the date when locoregional recurrence or distant metastasis was diagnosed. Overall survival and disease-free survival probabilities were estimated by the Kaplan-Meier method, and the log-rank test was applied to assess the significance of differences among actuarial survival curves. Multivariate analysis was carried out using Cox proportional hazards model (stepwise forward selection). All variables presenting $P < .20$ on the univariate analysis were selected for building a multiple model. For all tests, type I error (α) was established as 0.05, and results were considered statistically significant when $P < .05$. All statistical analyses were performed with the STATA software (Intercooled Stata release 7.0; Stata Corporation, College Station, TX).

Results

Identification of Genes Reactivated by 5Aza-dC

To identify novel methylation-silenced genes in HNSCC cell lines, we treated the FaDu cell line with the demethylating agent 5Aza-dC and used a combination of RaSH and cDNA microarray analysis to identify genes reactivated on treatment. Initially, two RaSH cDNA libraries were constructed: one using cDNA prepared from the FaDu cell line treated with 5Aza-dC as tester and the mock-treated FaDu cell line as driver (5Aza-dC tester library) and the other using cDNA prepared from mock-treated FaDu cell line as tester and cDNA from the FaDu cell line treated with 5Aza-dC as driver (mock tester library; Figure 1). A total of 1773 cDNA clones were sequenced, corresponding to 876 and 897 clones derived from the 5Aza-dC tester and mock tester libraries, respectively. After similarity searches in public databases, we found that these sequences correspond to 415 known genes of which 65 were present in both RaSH libraries. A total of 181 and 169 genes were found exclusively in the 5Aza-dC tester and mock tester libraries, respectively. Of the 181 cDNA clones reactivated by the 5Aza-dC, 151 were successfully amplified and spotted onto glass slides (Figure 1; Table W1).

Microarray analysis was then carried out with RNA extracted from FaDu and three additional HNSCC cell lines (UM-SCC-14A, UM-SCC-17A, and UM-SCC-38A) derived from distinct topographical sites and treated with 5Aza-dC. Self-self experiments based on a statistical test for low-replication microarray studies were performed to
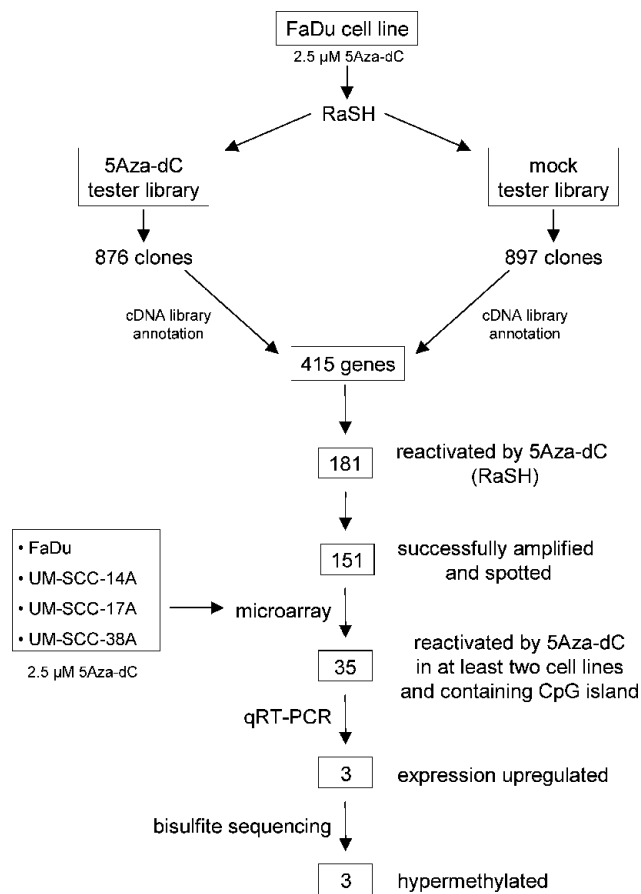
Figure 1. Flowchart for the identification of differentially methylated genes in HNSCC cell lines. FaDu cell line was treated with 5Aza-dC, and purified mRNA was used to construct RaSH cDNA libraries. A set of 151 nonredundant genes was used to prepare an enriched cDNA platform for microarray analysis. A total of 48 genes were reactivated in at least two cell lines. From them, 35 genes harboring a CpG island located at their 5′ region were submitted to qRT-PCR. Up-regulation of gene expression by 5Aza-dC was confirmed for three genes. Bisulfite sequencing revealed three differentially methylated genes.

identify genes reactivated on treatment. A total of 78 reactivated genes were identified using this combined approach, of which 31, 18, 47, and 46 were identified in the FaDu, UM-SCC-14A, UM-SCC-17A, and UM-SCC-38A cell lines, respectively. A total of 48 genes were reactivated in at least two cell lines and used for further investigation. We reasoned that commonly reactivated genes, inactivated in at least two HNSCC, were more likely to represent genes frequently inactivated in tumors.

Validation Analysis by qRT-PCR of Genes Reactivated by 5Aza-dC in HNSCC Cell Lines

Of the 48 genes selected by the microarray analysis, 35 harbored a bona fide CpG island in the 5′ region and were further selected for qRT-PCR quantification of gene expression in the same cell lines used in the microarray analysis (Table W2). Three genes (*CRABP2*, *MX1*, and *SLC15A3*) were confirmed to be reactivated at least three-fold in at least one of the cell lines after 5Aza-dC treatment. All these genes were upregulated in the FaDu cell line. In addition, the *CRABP2* and *MX1* genes were also upregulated in the UM-SCC-14A and UM-SCC-38A cell lines, respectively (Table 1).

DNA Methylation Analysis in HNSCC Cell Lines

The methylation status of the CpG island at the 5′ region site of the *CRABP2*, *MX1*, and *SLC15A3* genes was then investigated by bisulfite sequencing in HNSCC cell lines that showed induction of gene expression after 5Aza-dC treatment.

A significant reduction in the global methylation level (from 40.00% to 5.50%) of the 5′ region of *CRABP2* was observed in the FaDu cell line after treatment with the demethylating agent, which is in agreement with the 4.6-fold increase in the *CRABP2* messenger RNA (mRNA) level observed in this cell line treated with 5Aza-dC. Corroborating this result (Figure 2), reduction in the methylation levels was observed for almost all CpG dinucleotides analyzed.

A less pronounced reduction in the DNA methylation level of the *MX1* 5′ region was observed in the FaDu (from 27.70% to 12.70%) and UM-SCC-14A (from 7.80% to 1.02%) cell lines (Figure 2). The reduction was limited to dinucleotides 39 to 56 located within the first exon of the *MX1* gene. Reduction in the methylation levels of these specific dinucleotides was directly correlated with induction of gene expression on treatment observed in these cell lines, as measured by qRT-PCR (22.4-fold for FaDu and 4.5-fold for UM-SCC-14A), suggesting that these dinucleotides play a critical role in transcription regulation.

In the case of *SLC15A3* gene, an increase of 7.3- and 3.0-fold in its expression level was observed in the FaDu and UM-SCC-38A cell lines, respectively. However, a significant reduction (from 96.6% to 5.5%) in the DNA methylation level of the *SLC15A3* 5′ region was exclusively observed in the UM-SCC-38A cell line. These results suggest that other epigenetic mechanisms, such as histone modification, may also play a critical role in regulating the expression of the *SLC15A3* gene.

DNA Methylation Analysis in Primary HNSCC

We next sought to determine whether *CRABP2* and *MX1* hypermethylation, identified in the preceding experiments using cell lines, was also present in primary HNSCC. The methylation status of *SLC15A3* was not further investigated in primary tumors because

Table 1. Validation of Gene Expression Reactivation by Microarray Analysis and qRT-PCR in 5Aza-dC–Treated HNSCC Cell Lines.

Official Symbol	Microarray				qRT-PCR (Fold Change)			
	FaDu	UM-SCC-14A	UM-SCC-17A	UM-SCC-38A	FaDu	UM-SCC-14A	UM-SCC-17A	UM-SCC-38A
CRABP2	Up	Up	Up	—	4.6	1.9	1.7	ND
MX1	Up	Up	—	Up	22.4	4.5	ND	0.2
SLC15A3	Up	Up	Up	Up	7.3	2.2	1.0	3.0

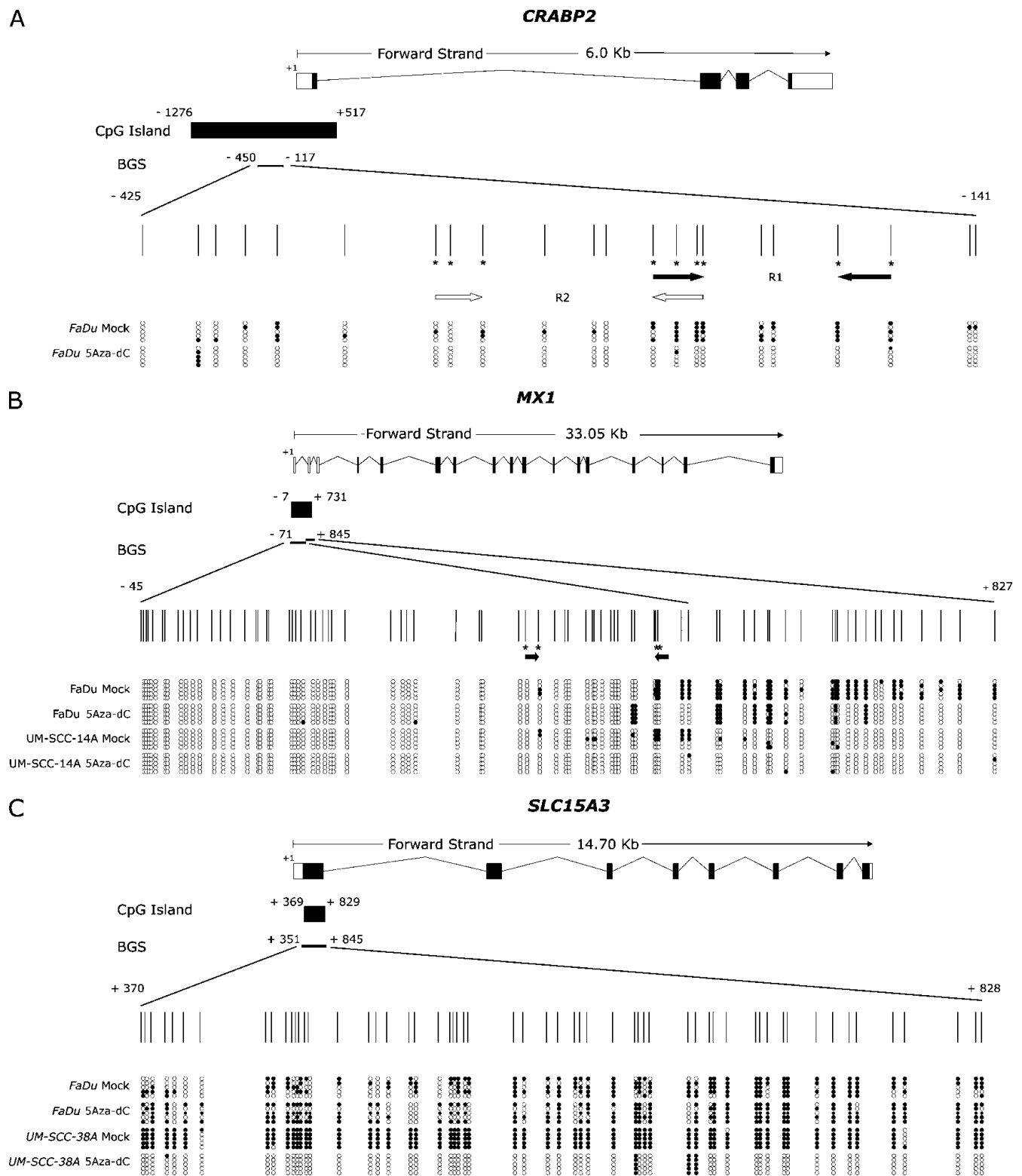*ND* indicates not determined; *Up*, upregulated.

Figure 2. A representative result of bisulfite sequencing. Each panel represents a schematic representation of the genome structure of each gene including their 5′ CpG islands. Exons and untranslated regions are represented by filled or open boxes, respectively. The transcription initiation site is represented by +1. Expanded view shows the position of CpG islands and the region analyzed by bisulfite sequencing. Vertical marks represent individual CpG dinucleotides and their spacing accurately reflects the CpG density of the region. MSP primers are represented by horizontal arrows in the panels. Primer sets M and U were designed for the same CpG dinucleotide (indicated by an asterisk). Methylation profiles of the treated (5Aza-dC) and untreated (mock) cell lines are indicated in the lower part of the panels. Each row represents one sequenced clone, and open and filled circles represent unmethylated and methylated CpG dinucleotides, respectively. (A) Bisulfite sequencing of *CRABP2* in the FaDu cell line. (B) Bisulfite sequencing of *MX1* in the FaDu and UM-SCC-14A cell lines. (C) Bisulfite sequencing of *SLC15A3* in the FaDu and UM-SCC-38A cell lines.
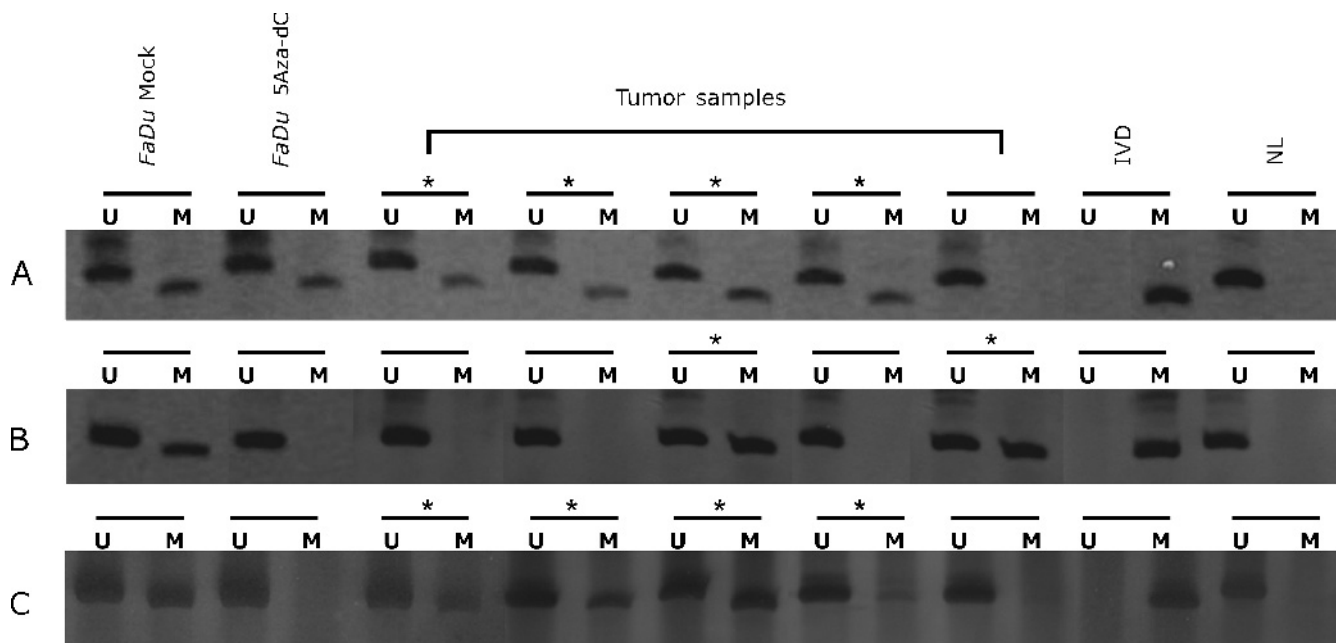
Figure 3. MSP analysis of *CRABP2* and *MX1* genes. Representative results of MSP analysis of *CRABP2* and *MX1* genes in the FaDu cell line and five different HNSCC samples. Methylated tumors are indicated with asterisks. The lanes indicated by M and U correspond to the products amplified by MSP primer sets specific for methylated and unmethylated DNA, respectively. *In vitro* methylated DNA (IVD) and normal human peripheral lymphocytes (NL) were used as positive and negative methylation controls, respectively. (A) MSP of *CRABP2* R1. (B) MSP of *CRABP2* R2. (C) MSP of *MX1*.

we were unable to detect a direct correlation between DNA methylation level and gene expression. MSP analysis of *CRABP2* and *MX1* was carried out in 140 HNSCC samples and 10 lymphocyte samples from normal individuals. The main clinicopathological characteristics of the HNSCC patients are shown in supplementary data (Table W3), and representative MSP results are shown in Figure 3. MSP primers were designed to target the most frequently methylated CpG dinucleotides and those with a direct correlation with mRNA expression as revealed by bisulfite sequencing of the tumor cell lines. Two primer pairs were designed for MSP analysis of the *CRABP2* (one

pair for region 1 – R1 and one pair for region 2 – R2) and a single primer pair was used for the *MX1* gene, as indicated in Figure 2.

CRABP2 hypermethylation was detected in 56.4% (79/140) of the samples when primers for R1 were used and in 10.0% (14/140) of the samples when reactions were carried out with R2 primers. For 13 patients (9.3%), hypermethylation was detected with both primer pairs. No *CRABP2* hypermethylation was detected in normal lymphocytes for both primer pairs. We then investigated the association between *CRABP2* hypermethylation and well-established clinicopathological parameters used for HNSCC. As shown in Table 2,

Table 2. Relationship between Methylation Analyses of *CRABP2* and *MX1* and Clinicopathological Variables in HNSCC Patients.

Variables	Category	*CRABP2* R1,* n (%)			*CRABP2* R2,* n (%)			*MX1,* n (%)		
		Unmethylated	Methylated	P	Unmethylated	Methylated	P	Unmethylated	Methylated	P
Age	≤53	26 (44.07)	23 (29.49)	.078	47 (38.52)	2 (14.29)	.074	29 (40.85)	20 (30.30)	.198
	>53	33 (55.93)	55 (70.51)		75 (61.48)	12 (85.71)		42 (59.15)	46 (69.70)	
Tumor site	Oral cavity	29 (49.16)	34 (43.04)	.010[†]	58 (47.15)	4 (28.57)	.097	39 (54.17)	24 (36.36)	.095
	Larynx	15 (25.42)	8 (10.13)		22 (17.89)	1 (7.14)		9 (12.50)	14 (21.21)	
	Hypopharynx	15 (25.42)	37 (46.84)		43 (34.96)	9 (64.29)		24 (33.33)	28 (42.43)	
Tumor size	T1 + T2	14 (25.00)	20 (26.32)	.864	30 (25.42)	4 (30.77)	.676	13 (18.31)	21 (34.43)	.035[†]
	T3 + T4	42 (75.00)	56 (73.68)		88 (74.58)	9 (69.23)		58 (81.69)	40 (65.57)	
Lymph nodes	N0	10 (17.54)	16 (21.33)	.588	21 (17.80)	5 (38.46)	.076	15 (21.13)	11 (18.03)	.656
	N+	47 (82.46)	59 (78.67)		97 (82.20)	8 (61.54)		56 (78.87)	50 (81.97)	
Grade	1	11 (19.64)	25 (34.25)	.184	34 (29.57)	2 (15.38)	.595	21 (31.34)	15 (24.19)	.563
	2	36 (64.29)	39 (53.42)		65 (56.52)	9 (69.23)		36 (53.73)	39 (62.90)	
	3	9 (16.07)	9 (12.33)		16 (13.91)	2 (15.38)		10 (14.93)	8 (12.90)	
Vascular invasion	No	35 (60.34)	51 (68.92)	.305	76 (64.41)	10 (76.92)	.367	40 (57.14)	45 (72.58)	.055
	Yes	23 (39.66)	23 (31.08)		42 (35.59)	3 (23.08)		30 (42.86)	17 (27.42)	
Lymphatic permeation	No	49 (84.48)	64 (87.67)	.599	100 (84.75)	12 (100)	.145	57 (82.61)	56 (90.32)	.200
	Yes	9 (15.52)	9 (12.33)		18 (15.25)	0		12 (17.39)	6 (9.68)	
Perineural infiltration	No	27 (46.55)	42 (57.53)	.211	60 (51.28)	9 (69.23)	.219	38 (55.07)	31 (50.00)	.562
	Yes	31 (53.45)	31 (42.47)		57 (48.72)	4 (30.77)		31 (44.93)	31 (50.00)	

R1 indicates region 1; *R2*, region 2.
*Percentages considering cases with complete information.
[†]Statistically significant.

a statistically significant association was found between tumor site and *CRABP2* hypermethylation in region 1 (*P* = .010). It was observed that hypopharynx tumors showed a higher frequency of methylation (37/52 or 71.2%) when compared with the other tumor sites. Kaplan-Meier analysis was then used to estimate the relationship between the methylation status of the *CRABP2* gene with overall and disease-free survival. No difference in terms of overall or disease-free survival was observed between patients with or without *CRABP2* hypermethylation in their primary tumors.

Hypermethylation in the 5′ region of the *MX1* gene was detected in 45.0% (63/140) of the HNSCC patients. Similar to what was observed for *CRABP2*, no *MX1* hypermethylation was detected in normal lymphocytes. A statistically significant association was observed between *MX1* hypermethylation and tumor size (*P* = .035) and a marginal association with vascular invasion (*P* = .055; Table 2). However, as for *CRABP2*, no difference in terms of overall or disease-free survival was observed between patients that did or did not show *MX1* hypermethylation in primary tumors.

CRABP2 Protein Expression in HNSCC Primary Tumors

CRABP2 protein expression was then analyzed in HNSCC tumors by immunohistochemistry using a TMA containing 75 HNSCC samples. As shown in Figure 4*A*, CRABP2 protein immunostaining was detected in the morphologically normal epithelium samples used as controls, more intense staining being detected in the suprabasal (post-mitotic) epithelial cells. Among the 75 HNSCC samples, 8 cases (11%) were negative, 37 cases (51%) were weakly positive, and 28 cases (38%) were strongly positive (Figure 4, *B–D*). Two samples did not con-

tain representative sections of the tumor tissue and were not considered in the analysis. For all further analysis, weakly and strongly positive tumors were treated as a single group with positive CRABP2 protein expression.

We then analyzed the possible association between the expression of CRABP2 protein and clinicopathological variables. As shown in Table 3, a statistically significant association was observed between CRABP2 staining and increased tumor size (T3 + T4; *P* = .029) and absence of lymphatic permeation (*P* = .014). Univariate analysis was used to estimate the association between CRABP2 protein expression and overall or disease-free survival. No difference in terms of overall survival was observed with CRABP2 protein expression. Interestingly, our data show that an absence of CRABP2 expression was associated with a worse disease outcome because patients whose tumors were negative for *CRABP2* expression had a higher risk of locoregional recurrence or distant metastasis than patients with CRABP2-positive tumors (log-rank test, *P* = .0531; Figure 5). In the Cox regression univariate model, CRABP2 protein expression showed a protective hazard ratio of 0.40 (95% confidence interval, 0.1-1.0). However, in the multivariate analysis, CRABP2 protein expression was not shown to be an independent prognostic factor for disease-free survival owing to the small number of CRABP2-negative tumors or to the presence of confounding variables such as tumor size and site and the occurrence of lymphatic permeation.

Discussion

Treatment with 5Aza-dC in combination with histone deacetylase inhibitors has been widely used to reactivate epigenetically silenced
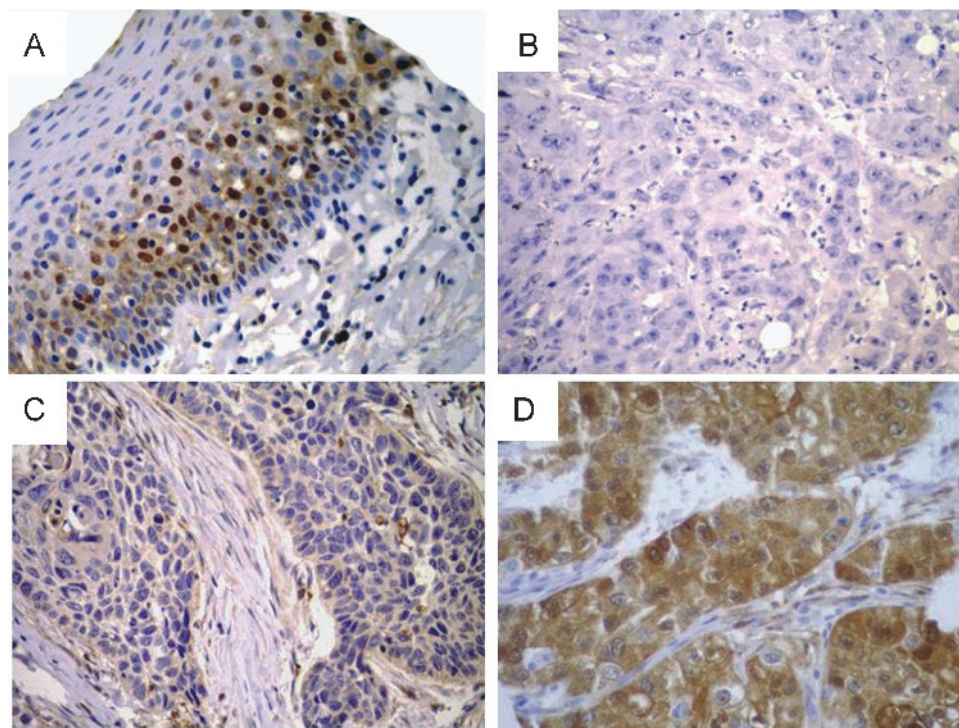

Figure 4. CRABP2 protein immunostaining patterns. Representative immunostainings of (A) morphologically normal epithelium and (B–D) HNSCC samples for CRABP2. Chromogenic detection (brown precipitate) counterstained with hematoxylin. Original magnifications: A, ×200 (A); B–D, ×400. Staining was scored as negative (B), weakly positive (C), or strongly positive (D).

Table 3. Relationship between CRABP2 Protein Expression and Clinicopathological Variables in HNSCC Patients.

Variables	Category	CRABP2,* n (%)		P
		Negative	Positive	
Age	≤53	1 (50.00)	13 (55.38)	>.999
	>53	7 (50.00)	52 (44.62)	
Tumor site	Oral cavity	3 (37.50)	20 (30.77)	NA
	Larynx	4 (50.00)	26 (40.00)	
	Hypopharynx	1 (12.50)	19 (29.23)	
Tumor size	T1 + T2	5 (71.43)	17 (29.82)	.029†
	T3 + T4	2 (28.57)	40 (70.18)	
Lymph nodes	N0	5 (62.50)	56 (91.80)	.075
	N+	3 (37.50)	5 (8.20)	
Histologic grade	1	3 (37.5)	22 (33.85)	NA
	2	5 (62.5)	36 (55.38)	
	3	0	7 (10.77)	
Vascular invasion	No	6 (75.00)	50 (80.65)	.707
	Yes	2 (25.00)	12 (19.35)	
Lymphatic permeation	No	2 (25.00)	43 (69.35)	.014†
	Yes	6 (75.00)	19 (30.65)	
Perineural infiltration	No	6 (75.00)	34 (54.84)	.278
	Yes	2 (25.00)	28 (45.16)	

NA indicates not applied.
*Percentages considering cases with complete information.
†Statistically significant.

genes in cell lines from several types of tumor [31–35]. Although this approach can lead to secondary effects on gene expression, it seems to be very efficient compared with alternative strategies in which CpG island arrays are hybridized with genomic DNA digested with methylation-sensitive restriction enzyme [15,36] because it relies directly on the reactivation of gene expression rather than on the presence of a CpG island.

In the present study, we have used 5Aza-dC to identify genes putatively silenced by DNA hypermethylation. Histone deacetylase inhibitors were not used because previous studies using similar strategies have demonstrated that most genes are reactivated by high-dose 5Aza-dC treatment, and only a small subset of genes is induced by the synergistic treatment with demethylating agents and deacetylase inhibitors [32,33].

To evaluate changes in gene expression induced by 5Aza-dC treatment, we used a combination of RaSH and cDNA microarray analysis. The RaSH methodology has been extensively used in the identification of differentially expressed genes, and in our study, it was used in an attempt to enrich the cDNA microarray for 5Aza-dC reactivated genes and not limit our analysis to a set of predefined genes represented in commercial arrays. Two RaSH cDNA libraries were constructed: 5Aza-dC tester and mock tester. The mock tester library was constructed in an attempt to identify false-positive genes that were found in both cDNA libraries and as a control of the subtraction efficiency. We identified 415 known genes of which only 65 were present in both RaSH libraries, indicating a high subtraction efficiency. In addition, we were able to identify 181 genes putatively induced by 5Aza-dC in the FaDu cell line, and 151 of these genes were spotted on the microarray platform and analyzed for gene reactivation in three additional HNSCC cell lines. Using this combined approach, we identified 78 genes induced on treatment and selected 35 genes, induced in at least two of the cell lines and which contained a CpG island at the 5′ region for technical validation by qRT-PCR. Gene expression increased at least three-fold on 5Aza-dC treatment in 3 of the 35 genes analyzed (*CRABP2*, *MX1*, and *SLC15A3*) and 2 of them (*CRABP2* and *MX1*) were indeed hypermethylated in the cell lines used in this study. MSP

was then used to examine the DNA methylation status of *CRABP2* and *MX1* in a set of 140 primary HNSCCs. MSP primers were designed to target the most frequently methylated CpG dinucleotides and those with a direct correlation with mRNA expression as revealed by bisulfite sequencing of the tumor cell lines. Because the CpG-rich region located at the 5′ region of *CRABP2* contains 22 CpG dinucleotides, two primer pairs (R1 and R2) were designed for MSP analysis of *CRABP2* in primary tumors. Unfortunately, owing to the higher GC content of the 5′ region of the *MX1* gene, we were able to design a single primer pair for MSP analysis of MX1. *CRABP2* hypermethylation was specifically detected in 56.4% and in 10.0% of the tumors when reactions were carried out with R1 and R2 primers, respectively. The difference in the methylation frequencies observed for different primer pairs is expected because MSP primers were placed at different CpG dinucleotides. *MX1* hypermethylation was specifically detected in 45.0% of primary HNSCCs. Taken together, these results suggest that *CRABP2* and *MX1* mRNA expression is regulated by DNA methylation and that *CRABP2* and *MX1* hypermethylation is frequent among HNSCCs. Interestingly, *CRABP2* (R1) or *MX1* hypermethylation showed statistically significant association with tumor site or tumor size, respectively. In the case of *CRABP2*, hypopharynx tumors showed a higher frequency of promoter methylation when compared with the other tumor sites.

The human *MX1* (myxovirus resistance 1) gene, also named IFI78 (interferon-inducible protein p78), encodes a member of the dynamin superfamily of large GTPases, which mediates vesicle trafficking and organelle homeostasis [37]. Similarly to other Mx proteins, human MX1 has antiviral activities against several RNA viruses and is transcriptionally induced by interferon through the JAK/STAT pathway [38]. *MX1* is upregulated in cells of some Fanconi anemia complementation groups, which may be related to phenotypic features of this disease, particularly bone marrow failure [23]. *MX1* is downregulated in prostate carcinomas [39] and methylated in acute myeloid leukemia cells [40], which provide a potential link between *MX1* silencing and tumorigenesis. Supporting this link are the observations by Mibayashi et al. [41] that MX1 promotes cell death induced by apoptotic stimuli. Therefore, low levels of MX1 protein might contribute to apoptosis resistance during cancer development.

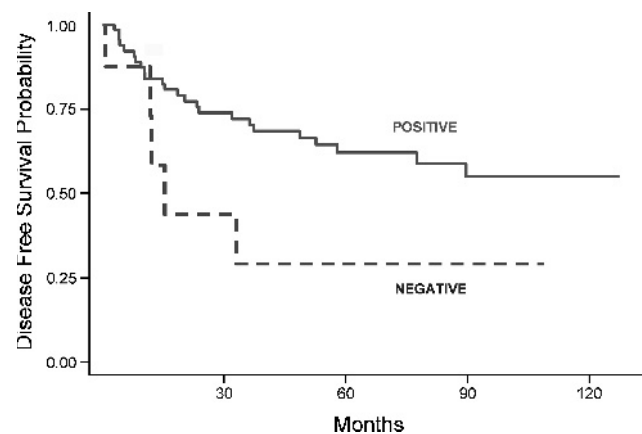
Figure 5. Kaplan-Meier disease-free survival estimates from 73 patients for CRABP2 expression. Continuous and dashed lines depict patients with positive (weak and strong) or negative CRABP2 expression (P = .0531), respectively.

CRABP2 (cellular retinoic acid binding protein 2) encodes a small protein (15 kDa) harboring a lipocalin domain involved in retinoic acid (RA) binding [42,43]. CRABP2 binds to all-*trans* RA in the cytoplasm, which triggers its nuclear targeting to associate with RA receptors (RARs). Owing to the poor water solubility of RA, its binding by CRABP2 allows the intracellular RA levels and availability to increase [44]. The association between CRABP2 and RAR in the nucleus enables direct channeling of RA and increases the RAR-RXR heterodimer transcriptional activity at RA-responsive sites [44].

RA and its derivatives (retinoids) are responsible for the regulation of multiple biologic processes, such as embryogenesis, apoptosis, cell proliferation, and differentiation [45]. Several authors have described retinoids as useful pharmaceuticals for the prevention and treatment of various types of human cancer. These studies demonstrated their efficiency in the treatment of tumors of head and neck [46,47], lung [48], skin [49], breast [50], and also of acute promyelocytic leukemia [51]. However, development of RA resistance frequently occurs [52]. Importantly, two major RA pathways were described as responsible for the antiproliferative and proliferative effects observed, respectively: the classic CRABP2/RAR and, more recently described, the FABP5/PPARβ/δ [53]. Therefore, both endogenous and exogenous retinoids may only inhibit tumor growth if the RAR pathway is predominant in the tumor cells, and this idea is supported by data showing that diverting RA from PPARβ/δ to RAR is sufficient to overcome RA resistance of mammary carcinomas [54]. In a related manner, abnormalities in the expression or in the function of retinoid receptors, particularly the suppression of RARB expression, have been found in several types of cancer, including premalignant oral lesions [55] and HNSCC [56,57]. Interestingly, *CRABP2* mRNA and protein levels were shown to be downregulated in carcinoma cells, relative to normal glandular cells, in the prostate [58,59]. Also, *CRABP2* was identified as downregulated in an oligomicroarray analysis of genes related to lymph node metastasis in esophageal squamous cell carcinoma [60]. More recently, *CRABP2* expression was demonstrated to be suppressed as a result of promoter DNA methylation in non–small cell lung tumor [61].

Finally, in confirmation that CRABP2 is an important component of the antiproliferative effects of the RAR pathway in response to RA, it was shown that CRABP2 induces apoptosis in MCF-7 mammary carcinoma cells because of the induction of transcription of cell cycle–regulating genes [62,63] and that overexpression of *CRABP2* in the HaCaT keratinocyte cell line significantly increased tumor necrosis factor α–induced apoptosis [53]. The correlation of *CRABP2* protein with the antiproliferative effect of RA and the induction of apoptosis in various cells are in agreement with the results of our study showing that *CRABP2* expression loss leads to survival disadvantage.

In the present study, we have demonstrated for the first time that *CRABP2* and *MX1* mRNA expression is regulated by DNA methylation and that hypermethylation of both genes is frequent among HNSCC. Although a direct correlation between *CRABP2* hypermethylatin and absence of protein expression was not directly evaluated in the present work, we observed similar frequencies for both CRABP2 hypermethylation (region 2 – 10.2%) and absence of CRABP2 protein (11.0%) in different sets of HNSCC samples, suggesting that DNA hypermethylation might also affect CRABP2 protein levels. Moreover, a statistically significant association between absence of CRABP2 protein and lower survival rates was observed in our study, suggesting that CRABP2 could be used as a prognostic biomarker for patients with HNSCC.

References

[1] McMahon S and Chen AY (2003). Head and neck cancer. *Cancer Metastasis Rev* **22**, 21–24.

[2] Goldenberg D, Lee J, Koch WM, Kim MM, Trink B, Sidransky D, and Moon CS (2004). Habitual risk factors for head and neck cancer. *Otolaryngol Head Neck Surg* **131**, 986–993.

[3] Parkin DM, Bray F, Ferlay J, and Pisani P (2005). Global cancer statistics, 2002. *CA Cancer J Clin* **55**, 74–108.

[4] Moriniere S (2006). Epidemiology of head and neck cancer [in French]. *Rev Prat* **56**, 1637–1641.

[5] Jemal A, Siegel R, Ward E, Murray T, Xu J, and Thun MJ (2007). Cancer statistics, 2007. *CA Cancer J Clin* **57**, 43–66.

[6] Brasil (2007). Estimativa 2008: Incidência de Câncer no Brasil. *Rio de Janeiro: Ministério da Saúde. Secretaria de Atenção à Saúde.* Brasil: Instituto Nacional do Câncer.

[7] Barnes L, Eveson JW, Reichart P, and Sidransky D (2005). *World Health Organization Classification of Tumors. Pathology and Genetics of Head and Neck Tumors.* Lyon, France: IARC Press.

[8] Ha PK and Califano JA (2006). Promoter methylation and inactivation of tumour-suppressor genes in oral squamous-cell carcinoma. *Lancet Oncol* **7**, 77–82.

[9] Shaw R (2006). The epigenetics of oral cancer. *Int J Oral Maxillofac Surg* **35**, 101–108.

[10] Hasegawa M, Nelson HH, Peters E, Ringstrom E, Posner M, and Kelsey KT (2002). Patterns of gene promoter methylation in squamous cell cancer of the head and neck. *Oncogene* **21**, 4231–4236.

[11] Calmon MF, Colombo J, Carvalho F, Souza FP, Filho JF, Fukuyama EE, Camargo AA, Caballero OL, Tajara EH, Cordeiro JA, et al. (2007). Methylation profile of genes *CDKN2A* (p14 and p16), *DAPK1*, *CDH1*, and *ADAM23* in head and neck cancer. *Cancer Genet Cytogenet* **173**, 31–37.

[12] Kozaki K, Imoto I, Mogi S, Omura K, and Inazawa J (2008). Exploration of tumor-suppressive microRNAs silenced by DNA hypermethylation in oral cancer. *Cancer Res* **68**, 2094–2105.

[13] Smith IM, Mydlarz WK, Mithani SK, and Califano JA (2007). DNA global hypomethylation in squamous cell head and neck cancer associated with smoking, alcohol consumption and stage. *Int J Cancer* **121**, 1724–1728.

[14] Richards KL, Zhang B, Baggerly KA, Colella S, Lang JC, Schuller DE, and Krahe R (2009). Genome-wide hypomethylation in head and neck cancer is more pronounced in HPV-negative tumors and is associated with genomic instability. *PLoS ONE* **4**, e4941.

[15] Costello JF, Fruhwald MC, Smiraglia DJ, Rush LJ, Robertson GP, Gao X, Wright FA, Feramisco JD, Peltomaki P, Lang JC, et al. (2000). Aberrant CpG-island methylation has non-random and tumour-type–specific patterns. *Nat Genet* **24**, 132–138.

[16] Esteller M (2007). Cancer epigenomics: DNA methylomes and histone-modification maps. *Nat Rev Genet* **8**, 286–298.

[17] Shames DS, Minna JD, and Gazdar AF (2007). Methods for detecting DNA methylation in tumors: from bench to bedside. *Cancer Lett* **251**, 187–198.

[18] Jones PA and Buckley JD (1990). The role of DNA methylation in cancer. *Adv Cancer Res* **54**, 1–23.

[19] Jiang H, Kang DC, Alexandre D, and Fisher PB (2000). RaSH, a rapid subtraction hybridization approach for identifying and cloning differentially expressed genes. *Proc Natl Acad Sci USA* **97**, 12684–12689.

[20] Ewing B, Hillier L, Wendl MC, and Green P (1998). Base-calling of automated sequencer traces using phred. I. Accuracy assessment. *Genome Res* **8**, 175–185.

[21] Ewing B and Green P (1998). Base-calling of automated sequencer traces using phred. II. Error probabilities. *Genome Res* **8**, 186–194.

[22] Smit AF (1999). Interspersed repeats and other mementos of transposable elements in mammalian genomes. *Curr Opin Genet Dev* **9**, 657–663.

[23] Altschul SF, Madden TL, Schaffer AA, Zhang J, Zhang Z, Miller W, and Lipman DJ (1997). Gapped BLAST and PSI-BLAST: a new generation of protein database search programs. *Nucleic Acids Res* **25**, 3389–3402.

[24] Gomes LI, Silva RL, Stolf BS, Cristo EB, Hirata R, Soares FA, Reis LF, Neves EJ, and Carvalho AF (2003). Comparative analysis of amplified and nonamplified RNA for hybridization in cDNA microarray. *Anal Biochem* **321**, 244–251.

[25] Maschietto M, de Camargo B, Brentani H, Grundy P, Sredni ST, Torres C, Mota LD, Cunha IW, Patrao DF, Costa CM, et al. (2008). Molecular profiling of isolated histological components of wilms tumor implicates a common role for the Wnt signaling pathway in kidney and tumor development. *Oncology* **75**, 81–91.

[26] Vencio RZ and Koide T (2005). HTself: self-self based statistical test for low replication microarray studies. *DNA Res* **12**, 211–214.

[27] Gardiner-Garden M and Frommer M (1987). CpG islands in vertebrate genomes. *J Mol Biol* **196**, 261–282.

[28] Pfaffl MW (2001). A new mathematical model for relative quantification in real-time RT-PCR. *Nucleic Acids Res* **29**, e45.

[29] Vandesompele J, De Preter K, Pattyn F, Poppe B, Van Roy N, De Paepe A, and Speleman F (2002). Accurate normalization of real-time quantitative RT-PCR data by geometric averaging of multiple internal control genes. *Genome Biol* **3**; RESEARCH0034.

[30] Herman JG, Graff JR, Myohanen S, Nelkin BD, and Baylin SB (1996). Methylation-specific PCR: a novel PCR assay for methylation status of CpG islands. *Proc Natl Acad Sci USA* **93**, 9821–9826.

[31] Liang G, Gonzales FA, Jones PA, Orntoft TF, and Thykjaer T (2002). Analysis of gene induction in human fibroblasts and bladder cancer cells exposed to the methylation inhibitor 5-aza-2′-deoxycytidine. *Cancer Res* **62**, 961–966.

[32] Suzuki H, Gabrielson E, Chen W, Anbazhagan R, van Engeland M, Weijenberg MP, Herman JG, and Baylin SB (2002). A genomic screen for genes upregulated by demethylation and histone deacetylase inhibition in human colorectal cancer. *Nat Genet* **31**, 141–149.

[33] Yamashita K, Upadhyay S, Osada M, Hoque MO, Xiao Y, Mori M, Sato F, Meltzer SJ, and Sidransky D (2002). Pharmacologic unmasking of epigenetically silenced tumor suppressor genes in esophageal squamous cell carcinoma. *Cancer Cell* **2**, 485–495.

[34] Sato N, Fukushima N, Maitra A, Matsubayashi H, Yeo CJ, Cameron JL, Hruban RH, and Goggins M (2003). Discovery of novel targets for aberrant methylation in pancreatic carcinoma using high-throughput microarrays. *Cancer Res* **63**, 3735–3742.

[35] Lodygin D, Epanchintsev A, Menssen A, Diebold J, and Hermeking H (2005). Functional epigenomics identifies genes frequently silenced in prostate cancer. *Cancer Res* **65**, 4218–4227.

[36] Wei SH, Chen CM, Strathdee G, Harnsomburana J, Shyu CR, Rahmatpanah F, Shi H, Ng SW, Yan PS, Nephew KP, et al. (2002). Methylation microarray analysis of late-stage ovarian carcinomas distinguishes progression-free survival in patients and identifies candidate epigenetic markers. *Clin Cancer Res* **8**, 2246–2252.

[37] Haller O, Staeheli P, and Kochs G (2007). Interferon-induced Mx proteins in antiviral host defense. *Biochimie* **89**, 812–818.

[38] Holzinger D, Jorns C, Stertz S, Boisson-Dupuis S, Thimme R, Weidmann M, Casanova JL, Haller O, and Kochs G (2007). Induction of *MxA* gene expression by influenza A virus requires type I or type III interferon signaling. *J Virol* **81**, 7776–7785.

[39] Schulz WA, Alexa A, Jung V, Hader C, Hoffmann MJ, Yamanaka M, Fritzsche S, Wlazlinski A, Muller M, Lengauer T, et al. (2007). Factor interaction analysis for chromosome 8 and DNA methylation alterations highlights innate immune response suppression and cytoskeletal changes in prostate cancer. *Mol Cancer* **6**, 14.

[40] Desmond JC, Raynaud S, Tung E, Hofmann WK, Haferlach T, and Koeffler HP (2007). Discovery of epigenetically silenced genes in acute myeloid leukemias. *Leukemia* **21**, 1026–1034.

[41] Mibayashi M, Nakad K, and Nagata K (2002). Promoted cell death of cells expressing human MxA by influenza virus infection. *Microbiol Immunol* **46**, 29–36.

[42] Astrom A, Tavakkol A, Pettersson U, Cromie M, Elder JT, and Voorhees JJ (1991). Molecular cloning of two human cellular retinoic acid–binding proteins (CRABP). Retinoic acid–induced expression of CRABP-II but not CRABP-I in adult human skin *in vivo* and in skin fibroblasts *in vitro*. *J Biol Chem* **266**, 17662–17666.

[43] Banaszak L, Winter N, Xu Z, Bernlohr DA, Cowan S, and Jones TA (1994). Lipid-binding proteins: a family of fatty acid and retinoid transport proteins. *Adv Protein Chem* **45**, 89–151.

[44] Budhu AS and Noy N (2002). Direct channeling of retinoic acid between cellular retinoic acid–binding protein II and retinoic acid receptor sensitizes mammary carcinoma cells to retinoic acid–induced growth arrest. *Mol Cell Biol* **22**, 2632–2641.

[45] De Luca LM (1991). Retinoids and their receptors in differentiation, embryogenesis, and neoplasia. *Faseb J* **5**, 2924–2933.

[46] Hong WK, Lippman SM, Itri LM, Karp DD, Lee JS, Byers RM, Schantz SP, Kramer AM, Lotan R, Peters LJ, et al. (1990). Prevention of second primary tumors with isotretinoin in squamous-cell carcinoma of the head and neck. *N Engl J Med* **323**, 795–801.

[47] Jetten AM, Kim JS, Sacks PG, Rearick JI, Lotan D, Hong WK, and Lotan R (1990). Inhibition of growth and squamous-cell differentiation markers in cultured human head and neck squamous carcinoma cells by β–all-*trans* retinoic acid. *Int J Cancer* **45**, 195–202.

[48] Pastorino U, Infante M, Maioli M, Chiesa G, Buyse M, Firket P, Rosmentz N, Clerici M, Soresi E, Valente M, et al. (1993). Adjuvant treatment of stage I lung cancer with high-dose vitamin A. *J Clin Oncol* **11**, 1216–1222.

[49] Kraemer KH, DiGiovanna JJ, Moshell AN, Tarone RE, and Peck GL (1988). Prevention of skin cancer in xeroderma pigmentosum with the use of oral isotretinin. *N Engl J Med* **318**, 1633–1637.

[50] Jing Y, Waxman S, and Mira-y-Lopez R (1997). The cellular retinoic acid binding protein II is a positive regulator of retinoic acid signaling in breast cancer cells. *Cancer Res* **57**, 1668–1672.

[51] Chomienne C, Fenaux P, and Degos L (1996). Retinoid differentiation therapy in promyelocytic leukemia. *FASEB J* **10**, 1025–1030.

[52] Garattini E, Gianni M, and Terao M (2007). Retinoids as differentiating agents in oncology: a network of interactions with intracellular pathways as the basis for rational therapeutic combinations. *Curr Pharm Des* **13**, 1375–1400.

[53] Schug TT, Berry DC, Shaw NS, Travis SN, and Noy N (2007). Opposing effects of retinoic acid on cell growth result from alternate activation of two different nuclear receptors. *Cell* **129**, 723–733.

[54] Schug TT, Berry DC, Toshkov IA, Cheng L, Nikitin AY, and Noy N (2008). Overcoming retinoic acid–resistance of mammary carcinomas by diverting retinoic acid from PPARβ/δ to RAR. *Proc Natl Acad Sci USA* **105**, 7546–7551.

[55] Hu L, Crowe DL, Rheinwald JG, Chambon P, and Gudas LJ (1991). Abnormal expression of retinoic acid receptors and keratin 19 by human oral and epidermal squamous cell carcinoma cell lines. *Cancer Res* **51**, 3972–3981.

[56] Zou CP, Clifford JL, Xu XC, Sacks PG, Chambon P, Hong WK, and Lotan R (1994). Modulation by retinoic acid (RA) of squamous cell differentiation, cellular RA-binding proteins, and nuclear RA receptors in human head and neck squamous cell carcinoma cell lines. *Cancer Res* **54**, 5479–5487.

[57] Youssef EM, Lotan D, Issa JP, Wakasa K, Fan YH, Mao L, Hassan K, Feng L, Lee JJ, Lippman SM, et al. (2004). Hypermethylation of the retinoic acid receptor-β(2) gene in head and neck carcinogenesis. *Clin Cancer Res* **10**, 1733–1742.

[58] Okuducu AF, Janzen V, Ko Y, Hahne JC, Lu H, Ma ZL, Albers P, Sahin A, Wellmann A, Scheinert P, et al. (2005). Cellular retinoic acid–binding protein 2 is down-regulated in prostate cancer. *Int J Oncol* **27**, 1273–1282.

[59] Thompson M, Lapointe J, Choi YL, Ong DE, Higgins JP, Brooks JD, and Pollack JR (2008). Identification of candidate prostate cancer genes through comparative expression-profiling of seminal vesicle. *Prostate* **68**, 1248–1256.

[60] Uchikado Y, Inoue H, Haraguchi N, Mimori K, Natsugoe S, Okumura H, Aikou T, and Mori M (2006). Gene expression profiling of lymph node metastasis by oligomicroarray analysis using laser microdissection in esophageal squamous cell carcinoma. *Int J Oncol* **29**, 1337–1347.

[61] Park JC, Chae YK, Son CH, Kim MS, Lee J, Ostrow K, Sidransky D, Hoque MO, and Moon C (2008). Epigenetic silencing of human T (brachyury homologue) gene in non–small-cell lung cancer. *Biochem Biophys Res Commun* **365**, 221–226.

[62] Donato LJ and Noy N (2005). Suppression of mammary carcinoma growth by retinoic acid: proapoptotic genes are targets for retinoic acid receptor and cellular retinoic acid–binding protein II signaling. *Cancer Res* **65**, 8193–8199.

[63] Donato LJ, Suh JH, and Noy N (2007). Suppression of mammary carcinoma cell growth by retinoic acid: the cell cycle control gene *Btg2* is a direct target for retinoic acid receptor signaling. *Cancer Res* **67**, 609–615.

Table W1. List of the 181 Reactivated Genes after 5Aza-dC Treatment Identified by RaSH cDNA Library.

Sequence	Official Symbol	CpG Island	Spotted in Array
CV341138	—	Yes	Yes
NM_000700	ANXA1	No	Yes
NM_001008897	TCP1	Yes	Yes
NM_002462	MX1	Yes	Yes
NM_005562	LAMC2	No	Yes
NM_005347	HSPA5	Yes	Yes
NM_004509	SP110	Yes	No
NM_005610	RBBP4	Yes	Yes
NM_001001977	ATP5E	Yes	Yes
NM_022073	EGLN3	Yes	Yes
NM_006476	ATP5L	Yes	Yes
NM_002893	RBBP7	Yes	No
NM_001799	CDK7	Yes	Yes
NM_016237	ANAPC5	Yes	Yes
NM_002463	MX2	Yes	Yes
NM_001852	COL9A2	Yes	No
NM_022121	PERP	Yes	Yes
NM_001012456	SEC61G	Yes	Yes
NM_002535	OAS2	Yes	No
NM_015013	AOF2	Yes	Yes
NM_006135	CAPZA1	Yes	Yes
NM_018835	RC3H2	Yes	No
NM_144596	TTC8	Yes	No
NM_002227	JAK1	No	Yes
NM_014352	POU2F3	Yes	Yes
NM_004923	MTL5	Yes	Yes
NM_003406	YWHAZ	Yes	Yes
NM_001007074	RPL32	Yes	Yes
NM_033407	DOCK7	Yes	No
NM_001686	ATP5B	Yes	Yes
NM_017688	BSPRY	Yes	Yes
NM_000979	RPL18	Yes	No
NM_005056	JARID1A	No	Yes
NM_020675	SPC25	Yes	Yes
NM_004371	COPA	Yes	No
NM_012420	IFIT5	Yes	Yes
NM_019606	MEPCE	Yes	Yes
NM_015091	FAM179B	Yes	Yes
NM_014612	FAM120A	Yes	No
NM_139266	STAT1	Yes	Yes
NM_014969	WDR47	Yes	Yes
NM_006004	UQCRH	Yes	Yes
NM_006819	STIP1	Yes	Yes
NM_004487	GOLGB1	Yes	Yes
NM_002421	MMP1	No	No
NM_006603	STAG2	Yes	Yes
NM_015340	LARS2	Yes	Yes
NM_000602	SERPINE1	No	Yes
NM_198076	FAM36A	Yes	Yes
NM_003746	DYNLL1	Yes	Yes
NM_005782	THOC4	Yes	Yes
NM_018660	ZNF395	Yes	Yes
NM_003792	EDF1	Yes	Yes
NM_005381	NCL	Yes	Yes
NM_005762	TRIM28	Yes	Yes
NM_002231	CD82	Yes	Yes
NM_002797	PSMB5	No	Yes
NM_001748	CAPN2	Yes	No
NM_001009925	C20orf30	Yes	Yes
NM_000646	AGL	Yes	Yes
NM_183356	ASNS	Yes	Yes
NM_005100	AKAP12	Yes	Yes
NM_006421	ARFGEF1	Yes	No
NM_198829	RAC1	Yes	Yes
NM_006931	SLC2A3	No	Yes
NM_000366	TPM1	Yes	Yes
NM_005365	MAGEA9	No	Yes
NM_006815	TMED2	Yes	Yes
NM_022754	SFXN1	Yes	Yes
NM_004755	RPS6KA5	Yes	Yes
NM_015382	HECTD1	Yes	No
NM_005243	EWSR1	Yes	Yes

Table W1. (*continued*)

Sequence	Official Symbol	CpG Island	Spotted in Array
NM_004130	GYG1	Yes	Yes
NM_153649	TPM3	Yes	Yes
NM_021101	CLDN	Yes	Yes
NM_006549	CAMKK2	Yes	Yes
NM_001175	ARHGDIB	No	Yes
NM_002673	PLXNB1	Yes	Yes
NM_198147	LOC116236	Yes	Yes
NM_014758	SNX19	Yes	Yes
NM_016565	CHCHD8	Yes	Yes
NM_020914	RNF213	Yes	No
NM_000576	IL1B	No	Yes
NM_005388	PDCL	Yes	No
NM_001080	ALDH5A1	Yes	Yes
NM_014611	MDN1	Yes	No
NM_015509	NECAP1	Yes	Yes
NM_003932	ST13	Yes	Yes
NM_002274	KRT13	No	Yes
NM_005789	PSME3	Yes	Yes
NM_182972	IRF2BP2	Yes	No
NM_004859	CLTC	Yes	Yes
NM_133337	FER1L3	Yes	Yes
NM_178868	CMTM8	Yes	Yes
NM_018043	ANO1	Yes	Yes
NM_003405	YWHAH	Yes	Yes
NM_016816	OAS1	Yes	Yes
NM_001457	FLNB	Yes	Yes
NM_003670	BHLHB2	Yes	Yes
NM_014014	ASCC3L1	Yes	No
NM_002094	GSPT1	Yes	No
NM_002080	GOT2	Yes	Yes
NM_005113	GOLGA5	Yes	Yes
NM_032547	SCOC	Yes	Yes
NM_000526	KRT14	No	No
NM_203459	CAMSAP1L	Yes	Yes
NM_030920	ANP32E	Yes	Yes
NM_015575	GIGYF2	Yes	Yes
NM_005744	ARIH1	Yes	Yes
NM_032565	EBPL	Yes	Yes
NM_177423	PPFIA1	Yes	Yes
NM_000989	RPL30	Yes	Yes
NM_014752	SPCS2	Yes	Yes
NM_201517	H2AFV	Yes	Yes
XM_031689	—	Yes	Yes
NM_031430	RILP	Yes	No
NM_213646	WARS	Yes	No
NM_001975	ENO2	Yes	No
NM_032940	POLR2C	Yes	Yes
NM_032366	C16orf13	Yes	Yes
NM_024881	SLC35E1	Yes	Yes
NM_005389	PCMT1	Yes	Yes
NM_020899	ZBTB4	Yes	Yes
NM_002822	TWF1	Yes	Yes
NM_016582	SLC15A3	Yes	Yes
NM_016286	DCXR	Yes	Yes
NM_001614	ACTG1	Yes	Yes
NM_001878	CRABP2	Yes	Yes
NM_144570	HN1L	Yes	Yes
NM_002272	KRT4	No	Yes
NM_001539	DNAJA1	Yes	Yes
NM_018156	VPS13D	Yes	Yes
NM_001005340	GPNMB	Yes	Yes
NM_003039	SLC2A5	Yes	Yes
NM_003467	CXCR4	Yes	Yes
NM_000661	RPL9	Yes	Yes
NM_014831	LBA1	Yes	No
NM_017830	OCIAD1	Yes	Yes
NM_007146	VEZF1	Yes	Yes
NM_016091	EIF3EIP	Yes	Yes
NM_001331	CTNND	Yes	No
NM_013230	CD24	Yes	Yes
NM_005556	KRT7	Yes	Yes
NM_002211	ITGB1	Yes	No
NM_031899	GORASP1	Yes	Yes

Table W1. (*continued*)

Sequence	Official Symbol	CpG Island	Spotted in Array
NM_003972	BTAF1	Yes	Yes
NM_016284	CNOT1	Yes	Yes
NM_006362	NXF1	Yes	Yes
NM_006018	GPR109B	No	Yes
NM_181777	UBE2A	Yes	Yes
NM_006306	SMC1A	Yes	Yes
NM_013236	ATXN10	Yes	Yes
NM_015384	NIPBL	Yes	Yes
NM_002828	PTPN2	Yes	No
NM_018127	ELAC2	Yes	Yes
NM_002880	RAF1	Yes	Yes
NM_001008493	ENAH	Yes	Yes
NM_025137	SPG11	Yes	Yes
BC038574	—	Yes	Yes
NM_003376	VEGFA	Yes	No
NM_001025	RPS23	Yes	No
CV571660	—	Yes	Yes
CV411881	—	Yes	Yes
AL523333	—	Yes	Yes
NM_005121	MED13	Yes	Yes
NM_016072	GOLT1B	Yes	Yes
NM_004966	HNRPF	Yes	Yes
NM_015630	EPC2	Yes	Yes
NM_001002857	ANXA2	Yes	Yes
NM_016520	C9orf78	Yes	Yes
NM_006472	TXNIP	No	Yes
NM_003324	TULP3	Yes	Yes
NM_201281	MTMR2	Yes	Yes
NM_006796	AFG3L2	Yes	Yes
NM_005358	LMO7	Yes	Yes
BC027471	—	Yes	Yes
BM685726	—	Yes	Yes
NM_182926	KTN1	Yes	Yes
NM_001087	AAMP	Yes	Yes
NM_001008844	DSP	Yes	Yes
AW105461	—	Yes	Yes

Table W2. Validation of Gene Expression Reactivation by qRT-PCR in 5Aza-dC–Treated HNSCC Cell Lines.

Official Symbol	Cell Lines			
	FaDu	UM-SCC-14A	UM-SCC-17A	UM-SCC-38A
AAMP	1.7	1.7	ND	ND
ACTG1	ND	ND	0.8	0.6
AFG3L2	ND	ND	1.0	0.5
ASNS	ND	ND	1.1	0.3
ATP5E	0.8	1.7	1.6	ND
ATXN10	ND	ND	0.9	0.4
CAPZA1	ND	2.5	1.7	ND
CLDN1	1.9	2.4	ND	ND
CRABP2	4.6	1.9	1.7	0.4
DCXR	ND	ND	1.3	1.1
EIF3EIP	ND	ND	1.0	0.8
EPC2	1.3	ND	ND	0.7
MEPCE	0.9	ND	1.5	1.7
GOT2	0.6	1.1	ND	ND
HNRPF	ND	ND	0.8	0.5
KTN1	ND	ND	1.2	2.7
MED13	1.3	1.8	ND	ND
MX1	22.4	4.5	ND	0.2
OCIAD1	1.1	ND	1.4	0.7
PCMT1	0.9	ND	1.2	ND
PERP	2.1	1.7	ND	ND
PLXNB1	1.8	ND	ND	0.3
PSME3	ND	ND	1.0	0.6
RAC1	1.3	ND	1.1	ND
RAF1	ND	ND	1.2	1.1
RPL30	ND	1.3	1.1	0.6
SFXN1	0.7	ND	1.3	0.6
SLC15A3	7.3	2.2	1.0	3.0
SPG11	1.0	2.0	1.0	ND
STAG2	1.4	ND	1.9	1.8
THOC4	ND	ND	0.8	0.8
TNRC15	0.8	ND	ND	0.7
UQCRH	ND	1.6	1.3	ND
WDR47	1.5	ND	1.6	0.4
YWHAH	ND	ND	0.9	1.0

ND indicates not determined.

Table W3. Distribution of the HNSCC Cases According to Demographic, Lifestyle, and Clinico-pathological Variables.

Variables	Category	TMA, n (%)	MSP, n (%)
Age	≤53	14 (19.18)	51 (36.43)
	>53	59 (80.82)	89 (63.57)
Tumor site	Oral cavity	23 (30.67)	64 (45.71)
	Larynx	31 (41.33)	24 (17.14)
	Hypopharynx	21 (28.00)	52 (37.14)
Tumor size	T1 + T2	22 (33.85)	34 (25.37)
	T3 + T4	43 (66.15)	100 (74.63)
Lymph nodes	N0	8 (11.43)	26 (19.40)
	N+	62 (88.57)	108 (80.60)
Grade	1	25 (34.24)	36 (27.48)
	2	41 (56.16)	77 (58.78)
	3	7 (9.60)	18 (13.74)
Vascular invasion	No	57 (79.17)	115 (86.47)
	Yes	15 (20.83)	18 (13.53)
Lymphatic permeation	No	46 (63.89)	87 (64.93)
	Yes	26 (36.11)	47 (35.07)
Perineural infiltration	No	40 (55.56)	69 (51.88)
	Yes	32 (44.44)	64 (48.12)

Table W4. Sequence and Concentration of the Primer Pairs Used in the qRT-PCR Validation of Gene Induction.

Official Symbol	Sense	Sequence (5′ → 3′)	µM
AAMP	Forward	CACCTTTGCATTGCACTCAG	0.4
	Reverse	TATGGCCTGCACACTCAAAG	
ACTG1	Forward	AGCCTTCCTTCCTGGGTATG	0.5
	Reverse	TGTTGGCGTACAGGTCTTTG	
AFG3L2	Forward	ACGAGGTGGCAAGAAAGATG	0.4
	Reverse	ATGACTCCACCCCAGAACAG	
ASNS	Forward	AAGACAGCCCCGATTTACTG	0.5
	Reverse	AGAGCCTGAATGCCTTCCTC	
ATP5E	Forward	TGGCAGCAACGTAAAAATTG	0.4
	Reverse	ACATGTGCCCACACATCTTC	
ATXN10	Forward	GCGAGTGGAACAGGAATCTC	0.5
	Reverse	AGTTCTGGGAAAGCATGCAC	
CAPZA1	Forward	TCGGATGAGGAGAAGGTACG	0.5
	Reverse	CCCTTCCCTGAGGAGATTG	
CLDN1	Forward	GGTGCAGAAGATGAGGATGG	0.4
	Reverse	CATTGACTGGGGTCATAGGG	
CRABP2	Forward	GACCTCGTGGACCAGAGAACTG	0.4
	Reverse	CCTGGTGCACACAACGTCAT	
DCXR	Forward	GGCCTTTGACAGATCCTTTG	0.5
	Reverse	AGCACTGGCTGGAGACATTC	
EIF3EIP	Forward	ACTACCAGGCCATCAAGGTG	0.5
	Reverse	GATGGCATCCTGGTAACGAC	
EPC2	Forward	GCAAGGACATGCCTGATCTC	0.4
	Reverse	TTGCTGTGCTGAAATTGCTC	
GOT2	Forward	AATGTTTGCCTCTGCCAATC	0.4
	Reverse	CATCCGCATCTTTGCAGAC	
HNRPF	Forward	GCCTGGTAGCAACAGAAACC	0.5
	Reverse	CAGGTGATCTTGGGTGTGG	
KTN1	Forward	GTTTCCCCAGAAACGGAGTC	0.5
	Reverse	TGTGAGCTGTTGGTTTACCG	
MED13	Forward	TGAAGAGCATATCACCCTTGC	0.4
	Reverse	TTGAATGCCTGTCCTGTGAG	
MEPCE	Forward	CAACCCTGGTCGTCGTATG	0.4
	Reverse	CTGGCTTCAATTGGATTCG	
MX1	Forward	CAATCAGCCTGCTGACATTG	0.4
	Reverse	TGTCTCCTGCCTCTGGATG	
OCIAD1	Forward	GAATGGGAGGGCTGATTTTC	0.4
	Reverse	TGCATTCTGCGAAGACTCTC	
PCMT1	Forward	CTACAGACCGCTCCCACTATG	0.6
	Reverse	GGAGCACTGATTGTTGCTTG	
PERP	Forward	TACGAGGAGGGCTGTCAGAG	0.4
	Reverse	GGCGAAGAAGGAGAGGATG	
PLXNB1	Forward	TGGTTGCAAGCCATCAGAG	0.4
	Reverse	CTCTTGCAGGAGGGTCTGG	
PSME3	Forward	CCAAGGAACCAAGGTGTTTG	0.5
	Reverse	TGGGAATCAGGAGCTGTACC	
RAC1	Forward	TGCTTTTCCCTTGTGAGTCC	0.4
	Reverse	ATGGGAGTGTTGGGACAGTG	
RAF1	Forward	GCCGAACAAGCAAAGAACAG	0.5
	Reverse	AACACTGCACAGCACTCTGG	
RPL30	Forward	CCTGGGGTACAAGCAGACTC	0.4
	Reverse	TGATGGACACCAGTTTTAGCC	
SFXN1	Forward	GCAAGTTGTCGTGTCCAGGATT	0.6
	Reverse	TTCCAAAGTGTTCATAATGAATGG	
SLC15A3	Forward	AAGCTCGCTCTCCAAAACTG	0.4
	Reverse	GCACATTGACGGTCTCTGG	
SPG11	Forward	TCTCCCCAGGATAAGTCCAG	0.4
	Reverse	GAGGGCTTCAGGGGAATATG	
STAG2	Forward	AAACCAAAAGCAAGGCAAAG	0.4
	Reverse	GGTTTTCCTCCTCCATTTCC	
THOC4	Forward	CTCAGACGCCGATATTCAGG	0.5
	Reverse	CTCAAAGTGCACGTCTGCTG	
TNRC15	Forward	CTCCAGGAGGAACCCCTTC	0.6
	Reverse	TCCTCCTCGTCCTGTCAATC	
UQCRH	Forward	CGGAGGAGCTCTTTGACTTC	0.5
	Reverse	TGCCCAGATGATGAAGACTG	
WDR47	Forward	CCAGGGGTACAAAACCTCAG	0.4
	Reverse	GATAGGCCTCTGTGCATCAAC	
YWHAH	Forward	GCGGTGACAGAGCTGAATG	0.5
	Reverse	TGGTTTTCTGCTCAATGCTG	